Latin American Journal of Solids and Structures
www.lajss.org

Buckling configurations and dynamic response of buckled Euler-Bernoulli beams with non-classical supports

Abstract

Exact solutions of buckling configurations and vibration response of post-buckled configurations of beams with non-classical boundary conditions (e.g., elastically supported) are presented using the Euler-Bernoulli theory. The geometric nonlinearity arising from mid-plane stretching (i.e., the von Kármán nonlinear strain) is considered in the formulation. The nonlinear equations are reduced to a single linear equation in terms of the transverse deflection by eliminating the axial displacement and incorporating the nonlinearity and the applied load into a constant. The resulting critical buckling loads and their associated mode shapes are obtained by solving the linearized buckling problem analytically. The buckling configurations are determined in terms of the applied axial load and the transverse deflection. The first buckled shape is the only stable equilibrium position for all boundary conditions considered. Then the pseudo-dynamic response of buckled beams is also determined analytically. Natural frequency versus buckling load and natural frequency versus amplitudes of buckling configurations are plotted for various non-classical boundary conditions.

Keywords

Analytical solutions; buckling analysis; Euler-Bernoulli beam theory; pseudo-dynamic analysis; von Kármán nonlinearity.

B. G. Sinir[a]
B. B. Özhan[b]
J. N. Reddy[c]

[a,b,c]Department of Mechanical Engineering Texas A&M University, College Station, TX 77843-3123, USA

[a]Department of Civil Eng. Celal Bayar University, 45140 Manisa, Turkey

[b]Department of Mechanical Engineering; Applied Mathematics and Computation Center, Celal Bayar University, 45140 Manisa, Turkey

[c]Corresponding author:
jnreddy@tamu.edu

Received 23.05.2014
Accepted 23.06.2014
Available online 17.08.2014

1 INTRODUCTION AND BACKGROUND

Beams are common structural elements in many engineering systems. Often beams are subjected to axial compressive loads, which cause them to buckle. Linear eigenvalue problems can be formulated to determine the buckling loads and buckling configurations for a variety of boundary conditions (see Reddy, 2004; 2007). In reality, beams subjected to axial loads develop axial internal forces that stretch the centroidal axis of the beam, resulting in the geometric nonlinearity that couples the axial displacement to the transverse displacement. Although onset of buckling does not imply total failure of the structure, the knowledge of the value of the load that initiates buck-

ling is of value in the design of engineering structures.

The study of buckling of beams has received considerable attention in the last decade. Nayfeh and Emam (2008) and Emam and Nayfeh (2009) have obtained exact solutions for the buckling configurations of beams under classical boundary conditions, while including the von Kármán nonlinearity. Both of these studies claim to have carried out post-buckling analysis of beams, but they are flawed because the equation they have employed is not applicable for post-buckling analysis, as explained by Shen (2011). Furthermore, Sınır et al. (2010) showed numerically that the buckling configurations of clamped-pinned beams presented by Nayfeh and Emam (2008) and Emam and Nayfeh (2009) are incorrect, and Sınır (2010) presented the correct ones.

Although there exist analytical solutions of linear buckling of beam–columns using the Euler-Bernoulli and Timoshenko beam theories for both isotropic and laminated composite beams for classical boundary conditions (i.e., a combination of hinged, clamped, and free boundary conditions; see Reddy, 2004; 2007), to the best of the authors' knowledge, analytical solutions of buckling as well as pseudo-dynamic response about buckled configurations of beam-columns considering the von Kármán nonlinearity are not available for non-classical (e.g., edges with elastic supports). In this study, we obtain analytical solutions for the buckling configurations and pseudo-dynamic response about buckled configurations of beams with a variety of non-classical boundary conditions using the Euler-Bernoulli beam theory. The critical buckling loads and their associated mode shapes are obtained analytically for buckled configurations first, and then pseudo-dynamic response about the buckled configurations is determined using a novel analytical method.

2 GOVERNING EQUATIONS

2.1 Displacements and Strains

The Euler-Bernoulli hypothesis of straight lines normal to the axis of the beam before deformation remain (a) straight after deformation, (b) inextensible, and (c) rotate as rigid lines to remain perpendicular the bent axis is satisfied by the following choice of the displacement field (see Reddy, 2004; 2007, and Figure 1)

$$\mathbf{u}(\mathbf{x}) = u_1(x,z)\hat{\mathrm{e}}_1 + u_3(x,z)\hat{\mathrm{e}}_3 \equiv u_x(x,z)\hat{\mathrm{e}}_x + u_z(x,z)\hat{\mathrm{e}}_z \tag{1}$$

with

$$u_x(x,z) = u(x) + z\theta_x, \quad u_z(x,z) = w(x), \quad \theta_x \equiv -\frac{dw}{dx} \tag{2}$$

The simplified Green-Lagrange strain tensor [i.e., $(\partial u_1/\partial x)^2 \approx 0, (\partial u_1/\partial z)^2 \approx 0$] is

$$\begin{aligned} &\boldsymbol{\varepsilon} = \varepsilon_{11}\ \hat{\mathrm{e}}_1\hat{\mathrm{e}}_1,\ \varepsilon_{11} = \varepsilon_{xx} = \varepsilon_{xx}^{(0)} + z\varepsilon_{xx}^{(1)} \\ &\varepsilon_{xx}^{(0)} = \frac{du}{dx} + \frac{1}{2}\left(\frac{dw}{dx}\right)^2,\ \varepsilon_{xx}^{(1)} = \frac{d\theta_x}{dx} \end{aligned} \tag{3}$$

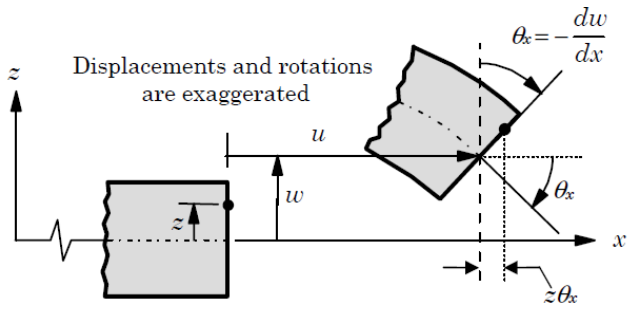

Figure1: Kinematics of the Euler–Bernoulli beam theory.

2.2 Equations of Motion

The equations of motion can be obtained using Hamilton's principle (see Reddy, 2004; 2007):

$$\int_{t_1}^{t_2} \left(-\delta K + \delta Q + \delta V \right) dt = 0 \tag{4}$$

where $-\delta K$ is the virtual kinetic energy, δQ is the virtual strain energy due to the actual internal forces moving through virtual displacements, and δV is the virtual work done by actual external forces, and δ denotes the variational operator. The equations of equilibrium are given by (Arbind et al., 2014; Reddy and Mahaffey, 2013)

$$\begin{aligned} -\frac{\partial M_{xx}^{(0)}}{\partial x} &= 0 \\ -\frac{\partial^2 M_{xx}^{(1)}}{\partial x^2} - \frac{\partial}{\partial x}\left(M_{xx}^{(0)} \frac{\partial w}{\partial x} - P\frac{\partial w}{\partial x} \right) - m_2 \frac{\partial^4 w}{\partial t^2 \partial x^2} + m_0 \frac{\partial^2 w}{\partial t^2} + \hat{\mu}\frac{\partial w}{\partial t} &= q \end{aligned} \tag{5}$$

where

$$\left(m_0, m_2 \right) = \int_A \rho \left(1, z^2 \right) dA \tag{6}$$

and

$$M_{xx}^{(0)} = \int_A \sigma_{xx}\, dA, \quad M_{xx}^{(1)} = \int_A z\sigma_{xx}\, dA \tag{7}$$

are the stress resultants, q is the distributed transverse load, ρ is density of the material, and P is the axial compressive load. The natural boundary conditions are to specify the following expressions [when the corresponding displacements are not specified]:

$$M_{xx}^{(0)}, \quad M_{xx}^{(0)}\frac{\partial w}{\partial x} - P\frac{\partial w}{\partial x} + \frac{\partial M_{xx}^{(1)}}{\partial x}, \quad M_{xx}^{(1)} \tag{8}$$

The stress resultants can be expressed in terms of the displacements by invoking the linear elastic constitutive relation, $\sigma_{xx} = E\varepsilon_{xx}$, where E is the modulus of elasticity. We have

$$\begin{Bmatrix} M_{xx}^{(0)} \\ M_{xx}^{(1)} \end{Bmatrix} = \int_A \begin{Bmatrix} \sigma_{xx} \\ z\sigma_{xx} \end{Bmatrix} dA = \int_A E \begin{Bmatrix} \varepsilon_{xx} \\ z\varepsilon_{xx} \end{Bmatrix} dA = \begin{Bmatrix} EA\left[\dfrac{\partial u}{\partial x} + \dfrac{1}{2}\left(\dfrac{\partial w}{\partial x}\right)^2\right] \\ EI\ \dfrac{\partial \theta_x}{\partial x} \end{Bmatrix} \tag{9}$$

where A is the cross-sectional area and I is the moment of inertia of the beam.

2.3 Elimination of the Axial Displacement

We note that the equations of equilibrium governing the axial displacement $u(x,t)$ and the transverse displacement $w(x,t)$ are coupled due to the von Kármán nonlinearity. Consequently, the equations cannot be solved analytically. In this section we discuss a strategy to eliminate the axial displacement $u(x,t)$ from the governing equations so that the von Kármán nonlinear term (in terms of the transverse deflection w) is absorbed into a constant, which enables analytical solution. We consider a beam of uniform cross-sectional area A, moment of inertia I, length l, constant modulus E, and subjected to a periodic transverse load

$$q = \hat{F}(x,t) \tag{10}$$

We make the following assumption (see Nayfeh and Pai, 2004): The beam is supported at the end points. Integrating the first equation in (5) with respect to x, we obtain

$$M_{xx}^{(0)} + C\left(t\right) = 0 \tag{11}$$

Where C is a time depentendent coefficient. Expressing eq. (11) in terms of the displacements, we obtain

$$\frac{\partial u}{\partial x} + \frac{1}{2}\left(\frac{\partial w}{\partial x}\right)^2 + \frac{1}{EA} C\left(t\right) = 0 \tag{12}$$

Integrating the above expression from 0 to l, we obtain the result

$$C = -\frac{EA}{2l}\int_0^l \left(\frac{\partial w}{\partial x}\right)^2 dx + \frac{EA}{l}\overline{u}\left(t\right) \tag{13}$$

where $\overline{u}\left(t\right) = u(0,t) - u(l,t)$. The negative value of $\overline{u}\left(t\right)$ means that beams gets longer. However, when the is subjected to a compressive load, $\overline{u}\left(t\right)$ is positive (i.e., the beam gets shorter). Using eq. (11)-(13) in the second equation of (10), we arrive at

$$-\rho I \frac{\partial^4 w}{\partial t^2 \partial x^2} + \rho A \frac{\partial^2 w}{\partial t^2} + \hat{\mu}\frac{\partial w}{\partial t} + EI\frac{\partial^4 w}{\partial x^4} + P\frac{\partial^2 w}{\partial x^2} - \frac{EA}{l}\frac{\partial^2 w}{\partial x^2}\left[\frac{1}{2}\int_0^l \left(\frac{\partial w}{\partial x}\right)^2 dx - \overline{u}\right] - \hat{F} = 0 \tag{14}$$

2.4. Nondimensionalized Equation

In the interest of convenience, we introduce the following non-dimensional quantities, and write eq. (14) in terms of the non-dimensional quantities:

$$\xi = \frac{x}{l}, \quad v = \frac{w}{r}, \quad U = \frac{\overline{u}}{l}, \quad r = \sqrt{\frac{I}{A}}, \quad \tau = \frac{t}{l^2}\sqrt{\frac{EI}{\rho A}},$$
$$\Lambda = \frac{Pl^2}{EI}, \quad \eta = \frac{l}{r}, \quad \mu = \frac{\hat{\mu} l^2}{\sqrt{\rho A EI}}, \quad F = \frac{\hat{F} l^4}{rEI} \tag{15}$$

In view of the non-dimensional quantities, the equation of equilibrium (14) reduces to

$$-\frac{1}{\eta^2}\frac{\partial^4 v}{\partial \tau^2 \partial \xi^2} + \frac{\partial^2 v}{\partial \tau^2} + \mu\frac{\partial v}{\partial \tau} + \frac{\partial^4 v}{\partial \xi^4} + \Lambda\frac{\partial^2 v}{\partial \xi^2} - \frac{\partial^2 v}{\partial \xi^2}\left[\frac{1}{2}\int_0^1 \left(\frac{\partial v}{\partial \xi}\right)^2 d\xi - \eta^2 U\right] - F = 0 \tag{16}$$

Eq. (16) is a nonlinear integro-differential equation. η is inverse of slenderness ratio and may be greater than 100. Thus, effects of the first term is getting disappear when increasing slender properties. On the other hand, importance of the axial deflection gets increase. So, we can say that the axial deflection has important effect on critical buckling load for highly slender beam.

2.5 Equation of Equilibrium

The equilibrium equation for buckling problem can be obtained by dropping the time dependent, damping, and forcing terms and denoting the buckled configuration by $v_s(\xi)$. The time dependent axial deflection, U, become a constant in spatial domain.

$$\frac{\partial^4 v_s}{\partial \xi^4} + \frac{\partial^2 v_s}{\partial \xi^2}\left[\Lambda - \frac{1}{2}\int_0^1 \left(\frac{\partial v_s}{\partial \xi}\right)^2 d\xi + \eta^2 U\right] = 0 \tag{17}$$

Eq. (17) is a linear, fourth-order, differential equation in v_s because of the fact that

$$\int_0^1 \left(\frac{dv_s}{d\xi}\right)^2 d\xi \tag{18}$$

and U are constants, although the former is not known. This equation is to be solved subject to various different boundary conditions. For hinged-hinged and clamped-clamped, and clamped-hinged boundary conditions, Nayfeh and Emam (2008) have presented the buckling solutions by assuming that $U = 0$. With this restriction, only onset of buckling can be predicted; post-buckling under applied in-plane load requires the movement of the end where the load is applied and, therefore $U \neq 0$. In addition, most designs of monolithic structures consider onset of buckling as a failure and, therefore, post-buckling becomes unimportant.

In the following section, analytical solutions for buckling, based on Eq. (17), are presented for non-classical boundary conditions that were not considered in the literature before.

3 ANALYTICAL SOLUTIONS FOR BUCKLING

3.1 General Solution

Eq. (16) simplifies for buckling analysis under axial load P as follows,

$$\frac{d^4 v_s}{d\xi^4} + \lambda^2 \frac{d^2 v_s}{d\xi^2} = 0 \ , \quad \lambda^2 = \Lambda - \frac{1}{2}\int_0^1 \left(\frac{\partial v_s}{\partial \xi} \right)^2 d\xi + \eta^2 U \tag{19}$$

The general solution to Eq. (19) is given by (see Reddy, 2004; 2007)

$$v_s(\xi) = c_1 \sin\lambda\xi + c_2 \cos\lambda\xi + c_3 \xi + c_4 \tag{20}$$

where (c_1, c_2, c_3, c_4) are constants to be determined using the boundary conditions, as discussed in the next two sections.

3.2 Boundary Conditions

Two types of non-classical boundary conditions are considered. The first one is termed *elastically hinged*, in which the beam is supported vertically by a linear elastic spring. Therefore, the vertical deflection in the spring is proportional to the vertical force, the proportionality constant is known as the extensional spring constant. The second type of non-classical boundary condition is called *elastically clamped*, in which the vertical deflection is zero but rotation is allowed in proportion to the moment. The proportionality constant in this case is the rotational spring constant. The solutions for these two types of boundary conditions are discussed first, followed by solutions for the four types of beams shown in Table 1.

***Elastically hinged edge* (*vertically spring-supported*):** In this case we have

$$v_s + \alpha \left(\frac{d^3 v_s}{d\xi^3} + \lambda^2 \frac{dv_s}{d\xi} \right) = 0 \ , \quad \frac{d^2 v_s}{d\xi^2} = 0 \quad \left(\alpha \geq 0 \right) \tag{21}$$

where α is the inverse of a non-dimensional elastic (spring) constant. When $\alpha = 0$ (i.e., the support is rigid), we recover the conventional simply supported boundary conditions that require the deflection and bending moment to be zero. When α is very large, the boundary condition approaches that of a free edge, requiring that the shear force and bending moment to be zero. Figure 2(a) shows the variation of λ with $1/\alpha$. For large values of $1/\alpha$, the solution asymptotically approaches the solution of the clamped-pinned (CP) type support.

***Elastically clamped edge* (*rotationally spring-supported*)**: For this case, we require

$$v_s = 0 \ , \quad \frac{dv_s}{d\xi} + \beta \frac{d^2 v_s}{d\xi^2} = 0 \quad \left(\beta \geq 0 \right) \tag{22}$$

where β is the inverse of the torsional spring constant. When $\beta = 0$ (i.e., the restraint is rigid), we recover the conventional clamped boundary conditions that the deflection and rotation be

zero. If β is very large (i.e., the restraint is very flexible), the condition approaches that of a simply supported case, where the deflection and bending moment are zero. Figure 2(b) shows the relationship between β and λ. Note that as $\beta \to 0$ we recover the result of the classical clamped-clamped (CC) boundary condition; and as $\beta \to \infty$, we recover the results of the clamped-pinned (CP) beam.

Clamped-elastically pinned 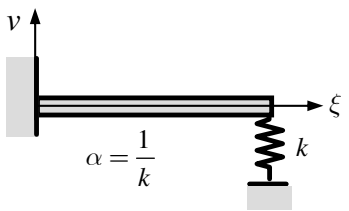	$\xi = 0$	$v_s = 0$
		$\frac{dv_s}{d\xi} = 0$
	$\xi = 1$	$\frac{d^2v_s}{d\xi^2} = 0$
		$v_s + \alpha\left(\frac{d^3v_s}{d\xi^3} + \lambda^2\frac{dv_s}{d\xi}\right) = 0$
Clamped-elastically clamped 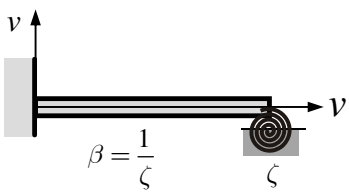	$\xi = 0$	$v_s = 0$
		$\frac{dv_s}{d\xi} = 0$
	$\xi = 1$	$v_s = 0$
		$\frac{dv_s}{d\xi} + \beta\frac{d^2v_s}{d\xi^2} = 0$
Pinned-elastically pinned 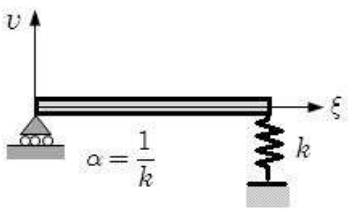	$\xi = 0$	$v_s = 0$
		$\frac{d^2v_s}{d\xi^2} = 0$
	$\xi = 1$	$\frac{d^2v_s}{d\xi^2} = 0$
		$v_s + \alpha\left(\frac{d^3v_s}{d\xi^3} + \lambda^2\frac{dv_s}{d\xi}\right) = 0$
Pinned-elastically clamped 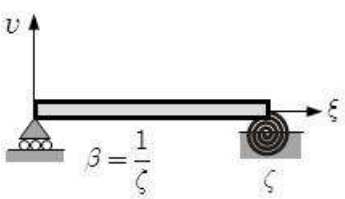	$\xi = 0$	$v_s = 0$
		$\frac{d^2v_s}{d\xi^2} = 0$
	$\xi = 1$	$v_s = 0$
		$\frac{dv_s}{d\xi} + \beta\frac{d^2v_s}{d\xi^2} = 0$

Table 1: Analyzed boundary conditions.

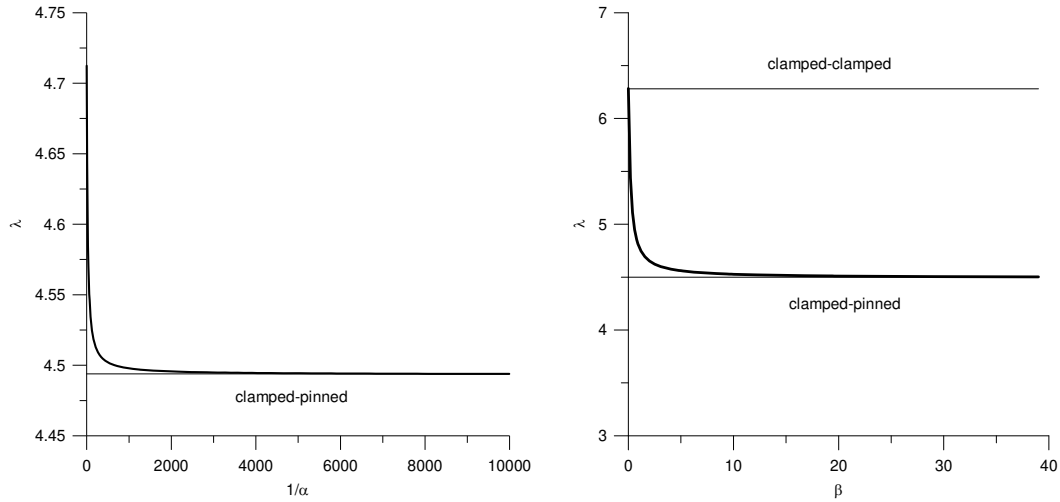

Figure 2: Plots of (a) $1/\alpha$ versus λ (clamped-clamped beam) and (b) β versus λ (clamped-pinned beam).

3.2.1 Clamped-Elastically Pinned Beam

For this case, we have $v_s = v_s' = 0$ at $\xi = 0$, and $v_s'' = 0$ and $v_s + \alpha\left(v_s''' + \lambda^2 v_s'\right) = 0$ at $\xi = 1$, where prime denotes the derivative with respect to coordinate ξ. Using these boundary conditions, we arrive at $c_2 + c_4 = 0$, $\lambda c_1 + c_3 = 0$, and

$$c_1 \sin\lambda + c_2 \cos\lambda = 0 \tag{23}$$

$$c_1 \sin\lambda + c_2 \cos\lambda + c_3\left(1 + \alpha\lambda^2\right) + c_4 = 0 \tag{24}$$

From these equations, we obtain $c_1 = -b_n \tan\lambda$, where $b_n \equiv c_2 = -c_4$. The buckling mode shape is

$$v_s = b_n\left[\cot\lambda\left(-\sin\lambda\xi + \lambda\xi\right) + \cos\lambda\xi - 1\right] \tag{25}$$

The case $\alpha = 0$, the characteristic equation corresponds to a CP beam. The case $\alpha = \infty$ corresponds to a clamped-free beam with the characteristic equation $\cos\lambda = 0$.

3.2.2 Clamped-Elastically Clamped Beam

For a beam clamped at one end and rotationally spring-supported (while prevented from moving vertically) at the other end is considered here. Using the boundary conditions $v = dv\,/\,d\xi = 0$ at $\xi = 0$, we obtain

$$c_2 + c_4 = 0 \tag{26}$$

$$\lambda c_1 + c_3 = 0 \tag{27}$$

Using the boundary conditions in Eq. (22), we obtain

$$c_1 \sin\lambda + c_2 \cos\lambda + c_3 + c_4 = 0 \tag{28}$$

$$\lambda\left(c_1\cos\lambda - c_2\sin\lambda\right) - \beta\lambda^2\left(c_1\sin\lambda + c_2\cos\lambda\right) + c_3 = 0 \tag{29}$$

Solving for the constants (c_1, c_3, c_4) in terms of $c_2 = b_n$, we obtain

$$c_1 = -b_n\frac{\cos\lambda - 1}{\sin\lambda - \lambda},\ c_3 = b_n\lambda\frac{\cos\lambda - 1}{\sin\lambda - \lambda},\ c_4 = -b_n \tag{30}$$

The characteristic equation for this case is

$$-2 + 2\cos\lambda + \lambda\sin\lambda + \lambda\beta\left(\lambda\cos\lambda - \sin\lambda\right) = 0 \tag{31}$$

and the eigenvector is

$$v_s = b_n\left[\frac{\cos\lambda - 1}{\sin\lambda - \lambda}\left(\lambda\xi - \sin\lambda\xi\right) + \cos\lambda\xi - 1\right] \tag{32}$$

When $\beta = 0$ we obtain $-2 + 2\cos\lambda + \lambda\sin\lambda = 0$, which is valid for a beam clamped both ends. When $\beta = \infty$ then eq. (29) reduces to $\lambda\cos\lambda - \sin\lambda = 0$, which corresponds to a beam clamped at one end pinned at the other end. For other values of the spring constant β, the value of λ and, hence, the critical buckling load, depends on β.

3.2.3 Pinned-Elastically Pinned Beams

For this case, the boundary conditions yield the relations

$$c_2 = 0\ ,\quad c_2 + c_4 = 0 \tag{33}$$

$$4\sin\lambda + c_2\cos\lambda = 0 \tag{34}$$

$$c_1\sin\lambda + c_2\cos\lambda + c_3\left(1 + \alpha\lambda^2\right) + c_4 = 0 \tag{35}$$

The solution of these equations is $c_2 = c_4 = 0$

$$c_3 = -b_n\frac{\sin\lambda}{1 + \alpha\lambda^2} \tag{36}$$

where $b_n \equiv c_1$. The characteristic equation becomes

$$\sin\lambda\left(1 + \alpha\lambda^2\right) = 0 \tag{37}$$

and the eigenvector is

$$v_s = b_n\left[\sin\lambda\xi - \frac{\sin\lambda}{1 + \alpha\lambda^2}\xi\right] \tag{38}$$

The case $\alpha = 0$ means pinned-pinned supports corresponds to a pinned-pinned (PP) beam and the case $\alpha = \infty$ is nonphysical.

3.2.4 Pinned-Elastically Clamped Beams

For this case, we have $c_2 = 0$ and $c_2 + c_4 = 0$

$$c_1 \sin\lambda + c_2 \cos\lambda + c_3 + c_4 = 0 \tag{39}$$

$$\lambda\left(c_1 \cos\lambda - c_2 \sin\lambda\right) + c_3 - \lambda^2\beta\left(c_1 \sin\lambda + c_2 \cos\lambda\right) = 0 \tag{40}$$

The characteristic equation is

$$\sin\lambda - \lambda\cos\lambda + \lambda^2\beta \sin\lambda = 0 \tag{41}$$

The case $\beta = 0$ corresponds to a CP beam with the characteristic equation, $\sin\lambda - \lambda\cos\lambda = 0$; and the case $\beta = \infty$ corresponds to a pinned-pinned (PP) beam with characteristic equation, $\sin\lambda = 0$, and the eigenvector $v_s\left(\xi\right) = b_n\left[\sin\lambda\xi - \xi\sin\lambda\right]$.

3.3 Numerical Results of Analytical Solution of Buckling

In this section, numerical results of buckling for four different non-classical boundary conditions are determined. Four parameters influence the behaviour of the beam: inverse of torsional spring coefficient (β), inverse of vertical spring coefficient (α), axial deflection (U), and slenderness ratio (η). In the following subsections, effects of these parameters is shown in detail. Numerical results indicate that there is no deflection up to the ciritical load. When the load reaches a critical value, the beam buckles. The region after the critical load is called the super-critical or post-buckling region. In this study, we do not show second and higher modes of buckling because the second buckled configuration is dynamically unstable (Nayfeh and Emam, 2008; Sinir, 2013). All plots are made for the point $\xi = 0.25$ along the beam.

3.3.1 Effects of β on Buckling

Recall that depending on the value of β, the elastically clamped support may be either clamped or pinned. The effect of β on buckling load and deflection is shown in Figure 3. The bifurcation diagram shows that the critical buckling load increases with decreasing β for a certain value of U and η. In other words, the stable region becomes larger with decreasing β (or increasing the support rigidity). In Figure 3a, the first curve is for PP beam and the last curve is for PC beam. Similiarly, in Figure 3b, the first and last curves denote deflections of CP and CC beams.

3.3.2 Effects of α on Buckling

In Figure 4, to show effects of inverse of vertical spring coefficient (α), the bifurcations diagrams are plotted only for the clamped-elastically pinned beam due to impractical application of pinned-elastically pinned beam. The bifurcation diagram shows that critical buckling load increases with increasing α (or decreasing vertical spring constant). The minimum critical load in the bifurcation diagram (Figure 4) corresponds to the critical buckling load of clamped-pinned beams.

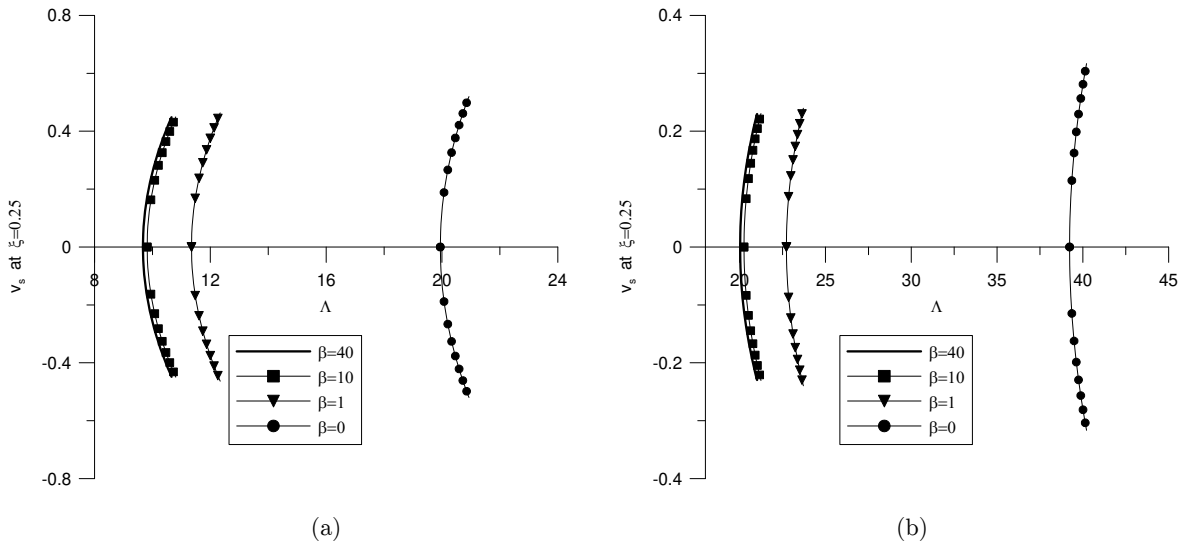

Figure 3: Effects of β on buckling for $U = 0.0001$ and $\eta = 50$ when the support is (a) pinned-elastically clamped (b) clamped-elastically clamped.

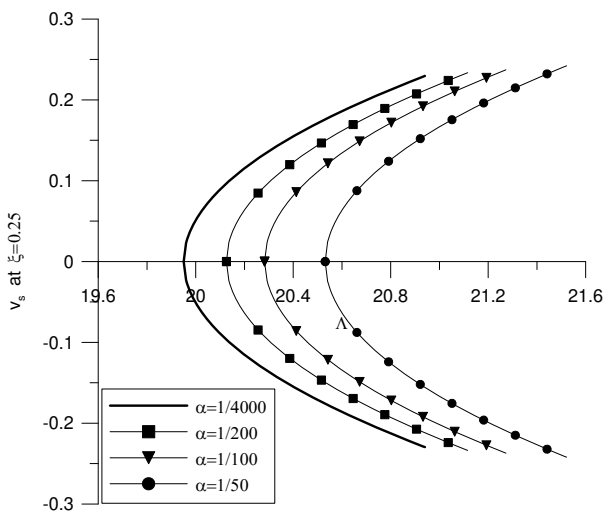

Figure 4: Effects of α on buckling for clamped-elastically pinned support when $U = 0.001$ and $\eta = 50$.

3.3.3 Effects of Axial Deflection U on Buckling

The solutions of the non-classical boundary conditions for clamped-clamped (CC), clamped-pinned (CP), pinned-pinned (PP) support conditions are presented in Figures 5a, 5b and 5c, respectively. Nayfeh and Emam (2008) obtained the critical buckling load and bifurcation diagrams without considering the axial deflection (i.e., they assumed $U = 0$).

The critical buckling load values are $4\pi^2, 2.05\pi^2, \pi^2$ for CC, CP and PP, respectively. The same results are obtained by using the non-classical boundary conditions. The buckling load is larger than the critical load. The effect of axial deflection on the critical buckling load is demonstrated clearly for the first time in the literature. The integral term in Eq. (19) arises from mid-

plane-stretching of the beam, making the beam stiffer. Therefore, the stretched beam can take larger load than the critical load. However, if an axial deflection (U) occurs, the load that the beam can take decreases, as can be seen from Figure 5. This has a practical importance. That is, if the beam is designed for large axial loads, the beam should not be allowed to experience axial movement (e.g., CC and PP beams).

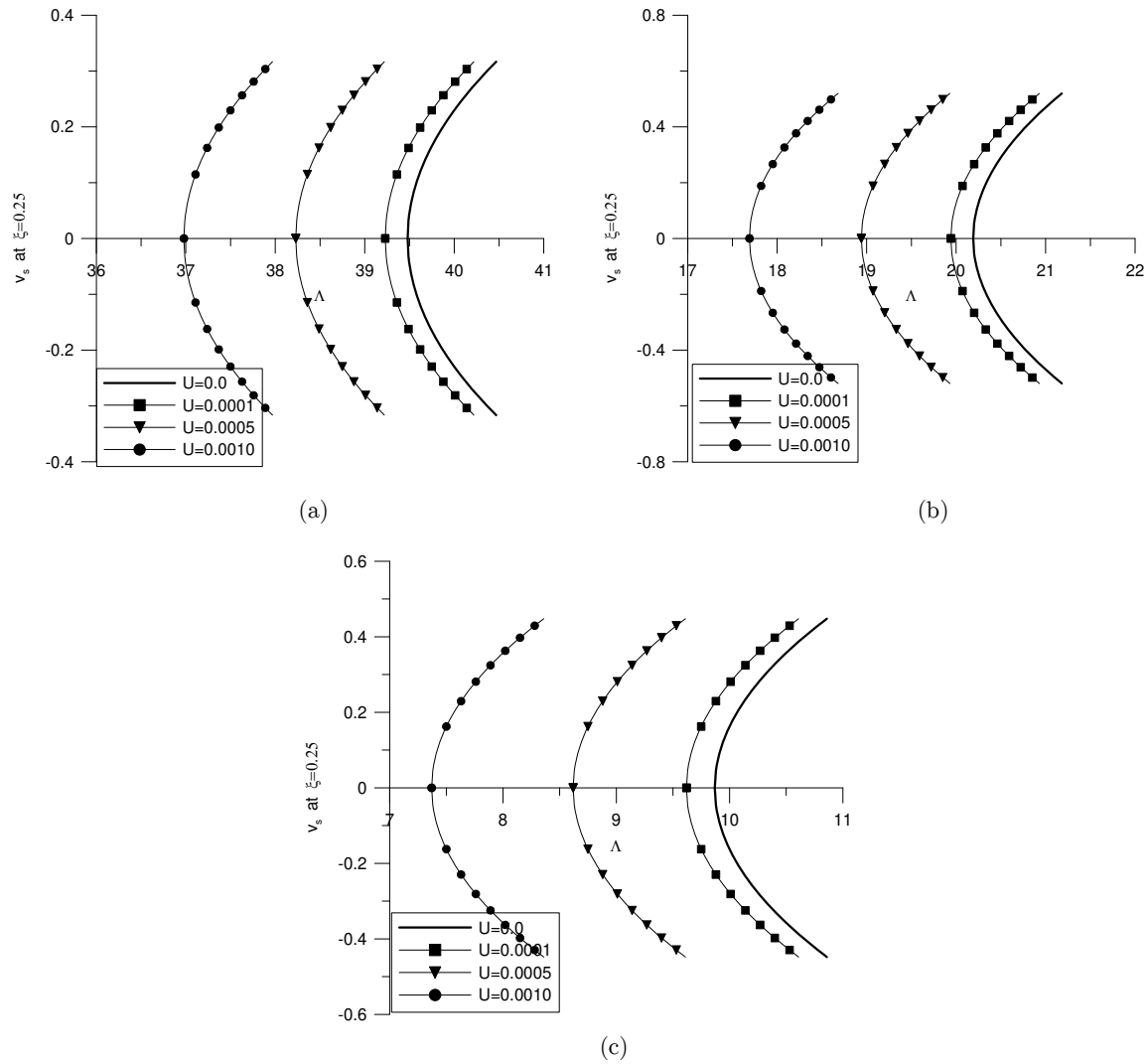

Figure 5: Effects of axial deflection, U on buckling for $\eta = 50$ when the support is (a) clamped-elastically clamped for $\beta = 0$ (clamped-clamped) (b) pinned-elastically clamped for $\beta = 0$ (pinned-clamped) (c) pinned-elastically pinned for $\alpha = 1/10000$ (pinned-pinned).

4 ANALYTICAL SOLUTION OF THE DYNAMIC RESPONSE

4.1 Governing Equations

The governing equation of motion of the Euler- Bernoulli beam in non-dimensional form is given by Eq. (16). Buckling is a static instability due to in plane axial compressive loads. To investigate

the dynamic stability of a buckled configuration, one can introduce a small disturbance and determine the time evolution of that disturbance. In this state, vibrations take place around a buckled configuration. In this section, the main objective is to investigate the significance of the axial load on the fundamental natural frequency of vibration, and to investigate the dynamic stability of a buckled configuration. Here we introduce different solution procedure than that of Nayfeh and Emam (2008) to determine the natural frequencies.

We first induce small change in the amplitude of the vibration mode, $v_d\left(\xi,\tau\right)$, around the buckled configuration,

$$v\left(\xi,\tau\right) = v_s\left(\xi\right) + v_d\left(\xi,\tau\right) \tag{42}$$

Substituting this equation into the equation of motion in Eq. (16), we obtain

$$\begin{aligned}&\frac{\partial^2 v_d}{\partial\tau^2} - \frac{r^2}{l^2}\frac{\partial^4 v_d}{\partial\xi^2\partial\tau^2} + \mu\frac{\partial v_d}{\partial\tau} + \frac{\partial^4 v_d}{\partial\xi^4} + \lambda^2\frac{\partial^2 v_d}{\partial\xi^2} - \frac{\partial^2 v_s}{\partial\xi^2}\int_0^1\left(\frac{\partial v_s}{\partial\xi}\frac{\partial v_d}{\partial\xi}\right)d\xi \\ &-\frac{\partial^2 v_s}{\partial\xi^2}\frac{1}{2}\int_0^1\left(\frac{\partial v_d}{\partial\xi}\right)^2 d\xi - \frac{\partial^2 v_d}{\partial\xi^2}\frac{1}{2}\int_0^1\left(\frac{\partial v_d}{\partial\xi}\right)^2 d\xi - \frac{\partial^2 v_d}{\partial\xi^2}\int_0^1\left(\frac{\partial v_s}{\partial\xi}\frac{\partial v_d}{\partial\xi}\right)d\xi = q\left(\xi\right)\cos\Omega\tau\end{aligned} \tag{43}$$

Note that this equation includes quadratic and cubic nonlinearities and harmonically varying external excitation, and its analytical solution is not possible. To investigate the fundamental natural frequencies (i.e., $q = 0$) and mode shapes of vibration in the vicinity of a buckled configuration, we consider only pseudo-nonlinear dynamic behavior of beams by dropping the damping term and all nonlinear terms.

4.2. The Pseudo-Nonlinear Dynamical Analysis

The pseudo-nonlinear vibrations problem is described the following equation:

$$\frac{\partial^2 v_d}{\partial\tau^2} - \eta^2\frac{\partial^4 v_d}{\partial\xi^2\partial\tau^2} + \frac{\partial^4 v_d}{\partial\xi^4} + \lambda^2\frac{\partial^2 v_d}{\partial\xi^2} - \frac{\partial^2 v_s}{\partial\xi^2}\int_0^1\frac{\partial v_s}{\partial\xi}\frac{\partial v_d}{\partial\xi}\,d\xi = 0 \tag{44}$$

In view of the fact the equation is linear; we can assume that the time variation is periodic

$$v_d(\xi,\tau) = X_m(\xi)\left(\mathrm{e}^{\mathrm{i}\omega_m\tau} + cc\right) \tag{45}$$

where $\mathrm{i} = \sqrt{-1}$, ω_m is the natural frequency, and cc denotes complex conjugate. The mode shape, $X_m(\xi)$, is not complex. The equation becomes

$$X_m^{iv} + \left(\eta^2\omega_m^2 + \lambda^2\right)X_m'' - \omega_m^2 X_m + \lambda^2\left(c_1\sin\lambda\xi + c_2\cos\lambda\xi\right)\int_0^1 v_s' X_m' d\xi = 0 \tag{46}$$

where the coefficients c_1, c_2, and buckled shape v_s depend on the boundary conditions. Eq. (46) is a non-homogenous ordinary differential equation; its solution consists of two parts: homogenous solution and the particular solution. The homogeneous solution is

$$X_{mh}\left(\xi\right)=\sum_{j=1}^{4}a_{j}e^{r_{j}\xi} \tag{47}$$

where r_j are found by solving the equation

$$r^{4}+\left(\lambda_{n}^{2}+\eta^{2}\omega_{m}^{2}\right)r^{2}-\omega_{m}^{2}=0 \tag{48}$$

Since the definite integral

$$h=\int_{0}^{1}X_{m}'v_{s}'\,d\xi \tag{49}$$

is a constant, the particular solution takes form,

$$X_{mp}\left(\xi\right)=A_{1}\sin\lambda\xi+A_{2}\cos\lambda\xi \tag{50}$$

where A_1 and A_2 are undetermined coefficients. Substituting Eq. (50) into Eq. (46) and solving for A_1 and A_2 we obtain

$$A_{1}=\frac{\lambda^{2}}{\omega_{m}^{2}\left(\lambda^{2}\eta^{2}+1\right)}c_{1}h\quad\text{and}\quad A_{2}=\frac{\lambda^{2}}{\omega_{m}^{2}\left(\lambda^{2}\eta^{2}+1\right)}c_{2}h \tag{51}$$

The complete solution is

$$X_{m}\left(\xi\right)=X_{mp}\left(\xi\right)+X_{mh}\left(\xi\right)=\sum_{j=1}^{4}a_{j}e^{r_{j}\xi}+\frac{\lambda^{2}h}{\omega_{m}^{2}\left(\lambda^{2}\eta^{2}+1\right)}\left(c_{1}\sin\lambda\xi+c_{2}\cos\lambda\xi\right) \tag{52}$$

where h is yet to be determined from Eq. (51). We have

$$\begin{aligned}h=\sum_{j=1}^{4}a_{j}\alpha_{j}\Bigg[1-\frac{\lambda^{3}}{\omega_{m}^{2}\left(\lambda^{2}\eta^{2}+1\right)}\Bigg(&\frac{c_{1}^{2}-c_{2}^{2}}{2}\cos\lambda\sin\lambda+c_{1}c_{2}\cos^{2}\lambda\\&+c_{3}\left(c_{1}\frac{\sin\lambda}{\lambda}+c_{2}\frac{\cos\lambda}{\lambda}\right)+\frac{\lambda}{2}\left(c_{1}^{2}+c_{2}^{2}\right)-c_{1}c_{2}-\frac{c_{2}c_{3}}{\lambda}\Bigg)\Bigg]^{-1}\end{aligned} \tag{53}$$

with

$$\begin{aligned}\alpha_{j}=\Bigg[&c_{3}\left(e^{r_{j}}-1\right)+c_{2}\frac{\lambda^{2}r_{j}}{\lambda^{2}+r_{j}^{2}}\left(e^{r_{j}}\left(\cos\lambda-\frac{r_{j}}{\lambda}\sin\lambda\right)-1\right)\\&+c_{1}\frac{\lambda r_{j}^{2}}{\lambda^{2}+r_{j}^{2}}\left(e^{r_{j}}\left(\cos\lambda+\frac{\lambda}{r_{j}}\sin\lambda\right)-1\right)\Bigg]\end{aligned} \tag{54}$$

To calculate the vibration mode shapes and frequencies of the buckled beam, we apply boundary conditions and obtain four algebraic equations in terms of a_1 , a_2 , a_3 , and a_4. These equations represent an eigenvalue problem for ω_m. Equating the determinant of the coefficient matrix of these equations to zero yields a fourth-order equation for ω_m^2. The roots of this equation, which are the eigenvalues of the coefficient matrix, are the natural frequencies of the buckled beam and the corresponding eigenvectors are the associated vibration mode shapes. The solutions procedure presented in this section is valid for all boundary conditions.

4.3. Numerical Results

4.3.1. Solution for a pinned-elastically pinned beam

As an example, we consider a pinned-elastically pinned beam due to its simplicity, to illustrate the procedure discussed. For this case, we obtain $c_1 = b_n$, $c_3 = -b_n \sin n\pi \Big/ \left(1 + \alpha n^2\pi^2\right)$ and $c_2 = c_4 = 0$. Using these relations and following the procedure outlined earlier, one can obtain mode shapes and natural frequencies of pinned-elastically pinned buckled beams as

$$A_1 = \frac{n^2\pi^2}{\omega_m^2\left(n^2\pi^2\eta^2 + 1\right)} b_n h \quad \text{and} \quad A_2 = 0 \tag{55}$$

$$\alpha_j = \left[b_n \frac{\sin n^2\pi^2}{1 + \alpha n^2\pi^2}\left(e^{r_j} - 1\right) + b_n \frac{n\pi r_j^2}{n^2\pi^2 + r_j^2}\left(e^{r_j}\left(\cos n\pi + \frac{n\pi}{r_j}\sin n\pi\right) - 1\right)\right] \tag{56}$$

$$h = \sum_{j=1}^{4} \frac{a_j\alpha_j}{1 - \dfrac{n^3\pi^3}{\omega_m^2\left(n^2\pi^2\eta^2 + 1\right)}\left(\dfrac{b_n^2}{2}\cos n\pi \sin n\pi - b_n \dfrac{\sin n\pi}{1 + \alpha n^2\pi^2}\left(b_n \dfrac{\sin n\pi}{n\pi}\right) + \dfrac{n\pi}{2} b_n^2\right)} \tag{57}$$

For the vibrations around the first buckled mode, the mode shape is

$$X_m\left(\xi\right) = \sum_{j=1}^{4} a_j e^{r_j\xi} + \frac{n^2\pi^2 h}{\omega_m^2\left(n^2\pi^2\eta^2 + 1\right)}\left(b_n \sin n^2\pi^2\xi\right) \tag{58}$$

Applying the boundary conditions, a set of algebraic equations are obtained (not presented here due to their algebraic complexity and without loss of information). This type of dynamic analysis is called post buckling analysis. In the following subsections, plots of natural frequency versus both buckling amplitude and axial load presented to show the effects of parameters β, α, U, η, b_n and Λ on natural frequencies.

4.3.1. Effects of Inverse of Torsional Spring Coefficient, β on Natural Frequency

In this study, two different boundary conditions, namely, clamped-elastically clamped and pinned-elastically clamped are considered. Depending on the value of the inverse of torsional spring coefficient, β, the clamped-elastically clamped beam may become either clamped-clamped beam $(\beta = 0)$ or clamped-pinned beam $(\beta \to \infty)$; the pinned-elastically clamped beam becomes

pinned-clamped beam or pinned–pinned beam. As can be seen from Figure 6a, the fundamental natural frequency increases with decreasing value of β. However, the second natural frequency essentially does not change for very small values of β, but for large values the frequency increases. In the plots of frequency versus axial load (see Figure 6b), the fundamental frequency increases with decreasing values of β up to a certain value of the axial load, and then the trend is reversed for higher axial loads. Nayfeh and Emam (2008) show that there is an intersection point between the first and the second natural frequencies for both clamped-clamped and pinned-pinned beams in contrast to clamped-pinned supports. This intersection point may lead to one-to-one internal resonance. Depending on the β values this intersection point may or may not exist.

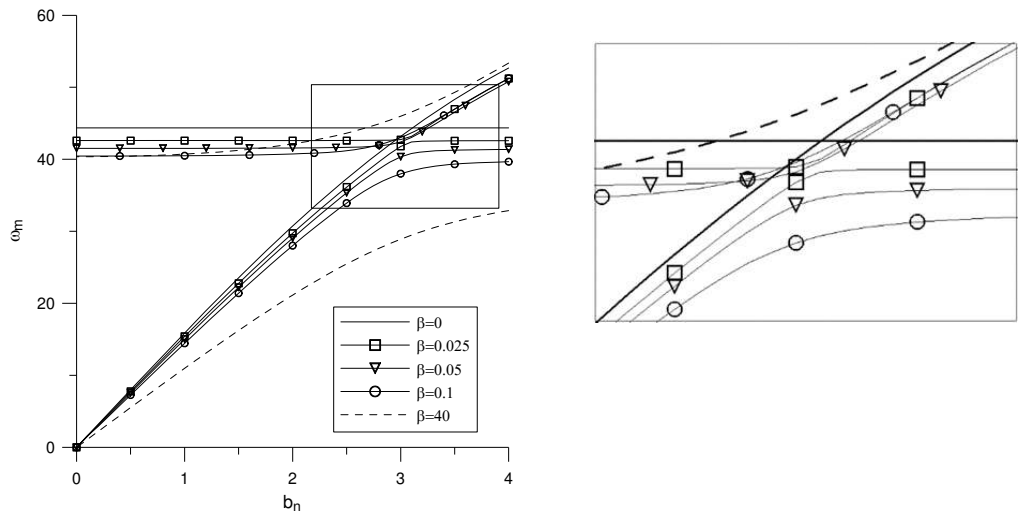

(a)

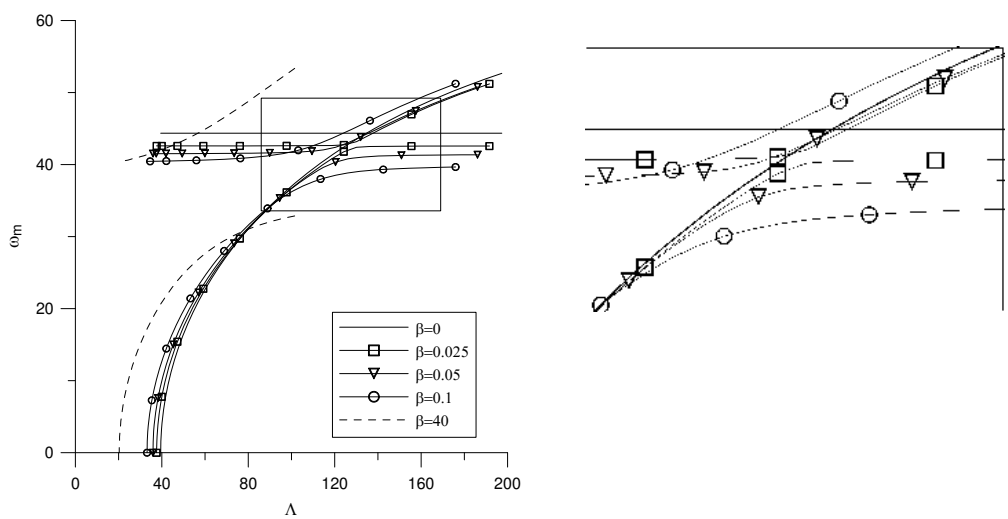

(b)

Figure 6: Effects of β on the natural frequencies (a) versus buckling amplitude and (b) versus axial load ($U = 0.0$) for clamped-elastically clamped beams.

Figure 7 contains plots similar to those in Figure 6, but for pinned-elastically clamped beam. In this case the trends reverse compared to those for the clamped-elastically clamped beam. This is expected because the beam becomes stiffer (and frequencies go up) with decreasing values of β.

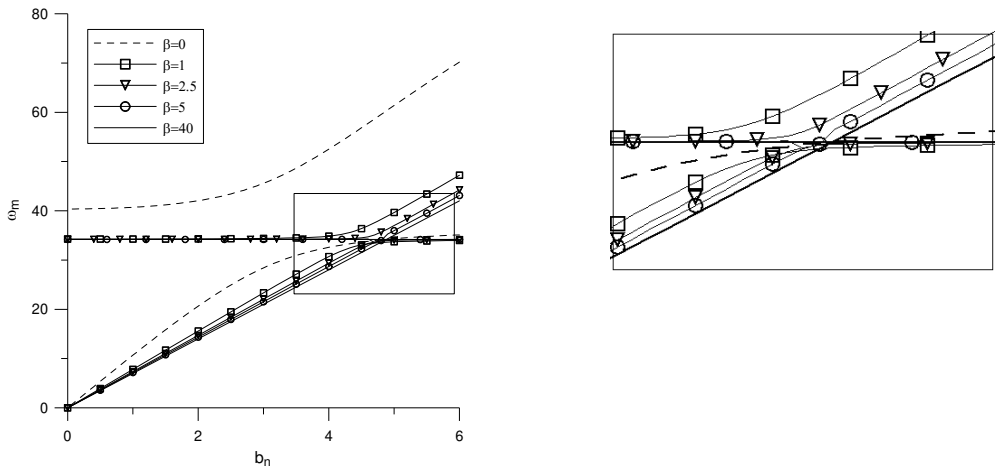

(a)

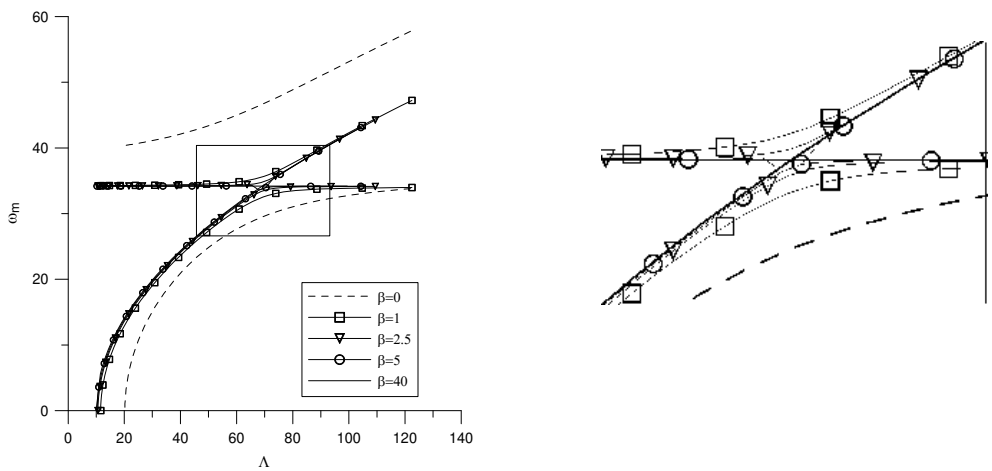

(b)

Figure 7: Effects of β values on natural frequencies (a) versus buckling amplitude (b) versus axial load ($U = 0.0$) for pinned-elastically clamped beams.

4.3.2. Effects of Inverse of Vertically Spring Coefficient of α on Natural Frequency

Figures 8a and 8b show the natural frequency versus buckling amplitude and natural frequency versus axial load, respectively, for clamped-elastically pinned beams. It can be seen from Figures 8a and 8b, that there are small differences in natural frequencies obtained with different values of α (the inverse of vertical spring constant). When the value of the vertical spring coefficient increases, the second mode natural frequencies also increase. Also, pinned-elastically pinned beam has no physical meaning for $\alpha = \infty$.

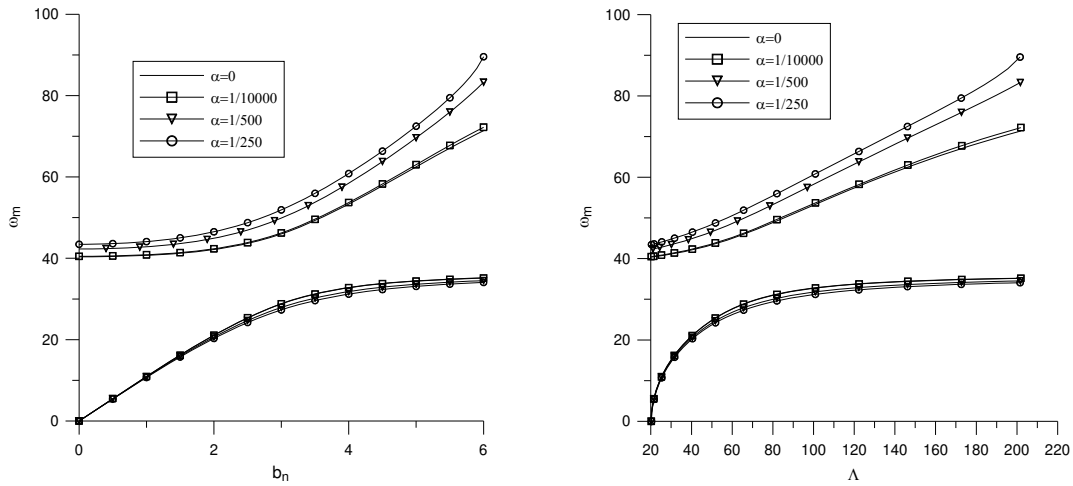

Figure 8: Effects of vertically spring coefficient on the natural frequency (a) versus buckling amplitude (b) versus axial load ($U = 0$) for clamped-elastically pinned beams.

4.3.3 Effects of Axial Deflection U on the Natural Frequency

The value of $U = [u(0,t) - u(l,t)] / l$ affects the axial load directly, If the axial deflection is allowed, then lower axial load can be obtained. In Figures 9a-9c, graphs of the natural frequency versus axial load are plotted to show the effect of axial deflection for classical boundary conditions (i.e., CC, PP, and PC). For CC and PP boundary conditions, the natural frequencies of vibration at the second mode are almost constant. Thus, the effect of axial deflection at the second mode for these boundary conditions disappears in contrast to the PC boundary condition. However, the effect of the axial deflection on the natural frequency can be seen at first mode vibration mode in vicinity of buckled beam.

4.3.4 Effects of Second Mode Buckling on Stability of the Beam

Another interesting case is the vibration about the second buckled configuration. In this case, the beam buckles at the second mode (see Figure 10). When the smallest frequency around the second buckled mode is calculated, the mode shape of the smallest frequency looks the same as the second mode shape. It is noted that the second mode is physically unstable.

5 SUMMARY AND CONCLUSIONS

In this study, exact solutions for the buckling configurations of beams with fixed/hinged and elastically supported ends using the Euler-Bernoulli theory with the von Kármán nonlinearity are presented. The governing equations are simplified by eliminating the axial displacement, while retaining the nonlinear term in the form of an unknown parameter. Analytical solutions for the buckling configurations of beams and the natural frequencies of vibration around the buckled beam are obtained for a variety of non-classical boundary conditions. The critical buckling loads

are obtained by solving the linear buckling problem analytically after incorporating the nonlinearity into a constant. The beam is stable at its original static equilibrium position, up to the first critical load, where it loses stability by a supercritical pitchfork bifurcation. Moreover, natural frequencies are obtained in post-buckling region about buckled configuration. Some interesting results are obtained for variety of non-classical boundary conditions. When the beam is elastically clamped, at certain spring values, the mode number of the calculated natural frequencies is not identifiable. It means that a calculated natural frequency for the spring coefficients may be for either first mode or second mode. The axial deflection and slenderness ratio have meaningful effects on the behavior of buckled beam. Extension of the present study using the Timoshenko beam theory is awaiting attention.

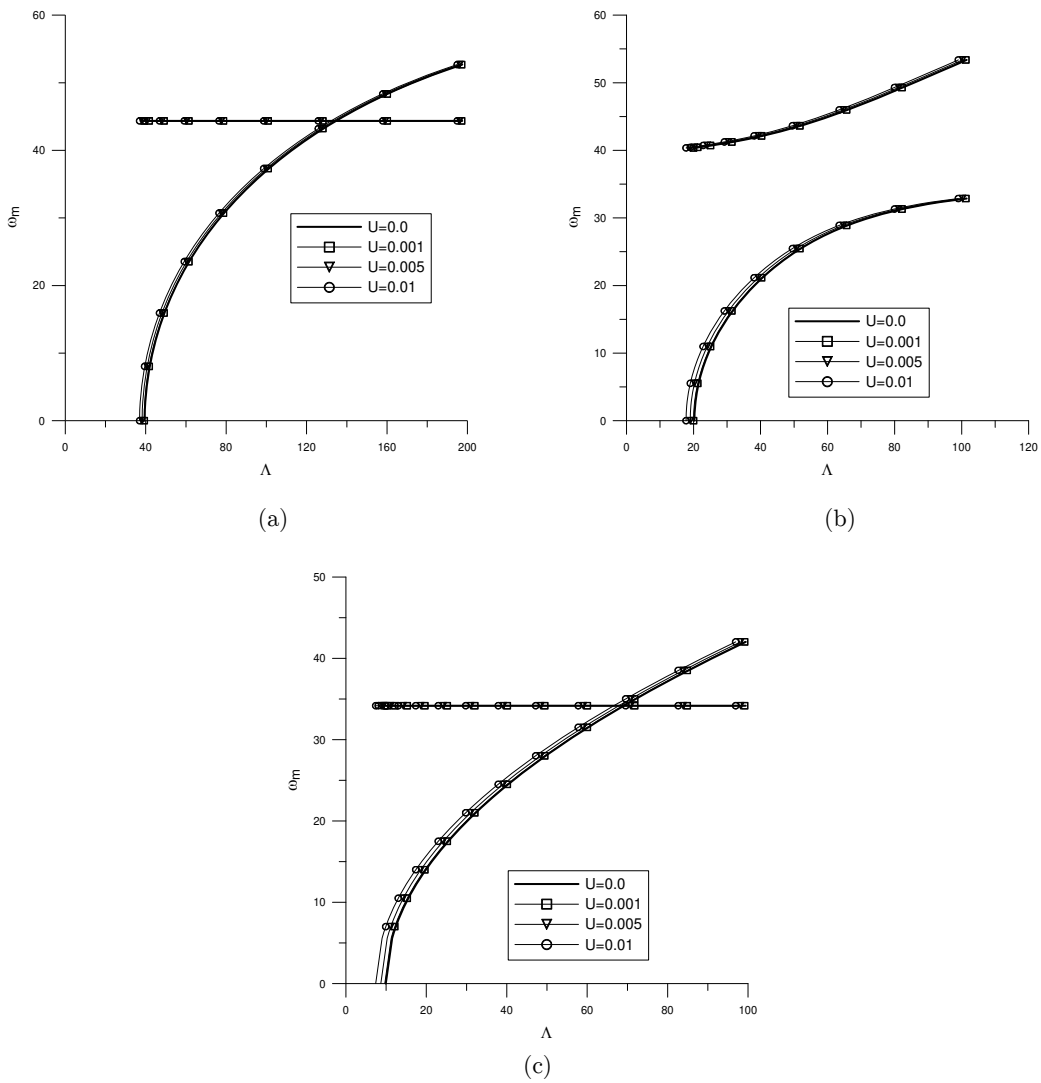

Figure 9: Effects of axial deflection, U on natural frequency for $\eta = 50$ when the support is (a) clamped-elastically clamped for $\beta = 0$ (clamped-clamped) (b) clamped-elastically clamped for $\beta = 40$ (clamped-pinned) (c) pinned-elastically clamped for $\beta = 40$ (pinned-pinned).

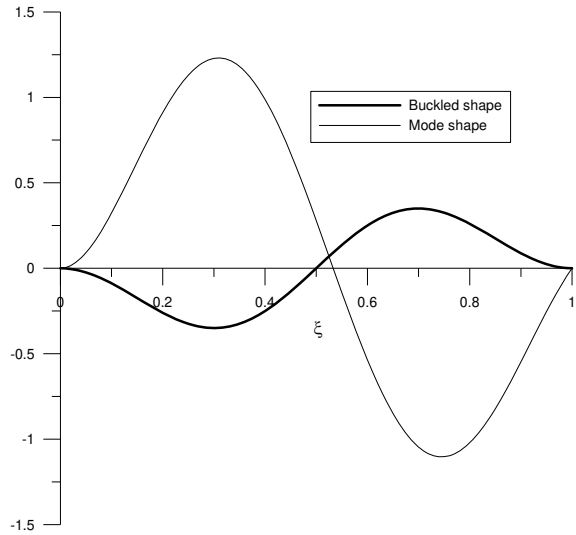

Figure 10: $\beta = 0$ (fixed-fixed beam), $c_n = 1.0$ and $\Lambda = 10.23$.

Acknowledgements

The first author acknowledges the support by National Science and Technology Foundation of Turkey (TÜBİTAK) and the second author acknowledges the support by Higher Education Council of Turkey (YÖK). The last author acknowledges the support of the research reported herein by the National Science Foundation research grants CMMI-1000790 and CMMI-1030836.

References

Arbind, A., Reddy, J.N., Srinivasa, A., (2014). Modified couple stress-based third-order theory for nonlinear analysis of functionally graded beams. Latin American Journal of Solids and Structures 11 (3): 459-487.

Emam, S.A., Nayfeh, A.H., (2009). Post-buckling and free vibrations of composite beams. Composite Structures, 88: 636-642.

Nayfeh, A.H., Emam, S.A., (2008). Exact solution and stability of postbuckling configurations of beams. Nonlinear Dynamics, 54: 395-408.

Nayfeh, A.H., Pai, P.F., (2004). Linear and Nonlinear Structural Mechanics. Wiley-Interscience, New York.

Reddy, J.N., (2004). Mechanics of Laminated Plates and Shells, Theory and Analysis, 2nd ed., CRC Press, Boca Raton, FL.

Reddy, J.N., (2007). Theory and Analysis of Elastic Plates and Shells, 2nd ed., CRC Press, Boca Raton, FL.

Reddy, J.N., Mahaffey, P., (2013). Generalized beam theories accounting for von Kármán nonlinear strains with application to buckling. Journal of Coupled Systems and Multiscale Dynamics, 1(1): 120-134.

Shen, H.S., (2011). A novel technique for nonlinear analysis of beams on two-parameter elastic foundation. International Journal of Structural Stability and Dynamics, 11(6): 999-1014.

Sinir, B.G., (2010). Bifurcation and chaos of slightly curved pipes. Mathematical and Computational Applications, 15(3): 490-502.

Sınır, B.G., (2013). Pseudo-nonlinear dynamic analysis of buckled pipes. Journal of Fluids and Structures, 37: 151–170.

Sinir, B.G., Değer, G., Tezcan, T., (2010). Approximate solution and stability of post-buckling configurations of beams using finite difference method. 9th International Congress on Advances in Civil Engineering, 27-30 September, 2010, Trabzon, Turkey.